Differential Geometric Methods for Jump Effects in Nonlinear Circuits

Tina Thiessen*, Martin Gutschke†, Philipp Blanke†, Wolfgang Mathis* and Franz-Erich Wolter†
*Institute of Theoretical Electrical Engineering, Email: thiessen@tet.uni-hannover.de
†Welfenlab – Division of Computer Graphics, Email: gutschke@gdv.uni-hannover.de
Leibniz University of Hanover, D-30167, Hanover, Germany

Abstract— **We present efficient algorithms for the simulation of problematic circuits with fast switching behavior based on the idea of tracing significant sets on the state space manifold. The switching behavior is represented by "jumps" from one part of the manifold to another. Our approach makes a regularization of the circuit unnecessary. In this article, we extend our approach to circuits with higher codimensions and jump spaces and verify the functionality by the application to a simple MOS flip flop. Furthermore, we show how to visualize the phenomena by using a special projection.**

I. Introduction

In previous works we have presented a differential geometric approach to compute the fast switching behavior of certain kinds of electronic circuits (cf. [1], [2], [3]). In our differential geometric view, the state space is a manifold embedded in the space of currents and voltages and fast switches are "jumps" through the embedding space from one point on the manifold to another one. We have shown (cf. [3]), that these jumps occur when the state space exhibits a fold with respect to a circuit specific projection direction. When simulating such circuits without regularization, the simulation fails because there are two or more states. One solution is to regularize the system's dynamics by manually introducing suitably located ϵ-parasitic L's and C's considering Tikhonov's Theorem [4]. The problem is, that choosing wrongly located L's and C's can lead to unreliable solutions. Another problem are the widely spaced time-constants which appear due to the fact that the dynamics of a regularized circuit can be divided into a slow and a fast part, leading to the so-called "time-constant problem" of circuit simulation. This difficulty can be circumvented by using stiff solvers (e.g. implicit integration methods like BDF or Gear method) if the reason for the time-constant problem is not related to a jump behavior [5].

In this work, we extend our concept to circuits with a higher dimensional embedding space examining the example of a MOS flip flop. Since this example exhibits a higher codimension of the state space manifold than previously considered circuits, we had to adapt our solving algorithms. In this work we show the applicability of our approach to higher dimensions and verify our results graphically and numerically by the classical approach of Tikhonov regularization.

II. Geometric Concept

Circuit equations can be considered as algebro-differential equations (DAEs) and by choosing a suitable chart, the system is described by eq. (1) and (2), cf. [3].

$$\boldsymbol{B}(\boldsymbol{x})\dot{\boldsymbol{x}} = \tilde{\boldsymbol{g}}(\boldsymbol{x},\boldsymbol{y},\boldsymbol{z}) \qquad \tilde{\boldsymbol{g}} : \mathbb{R}^k \to \mathbb{R}^n \quad (1)$$

$$\boldsymbol{0} = \boldsymbol{f}(\boldsymbol{x},\boldsymbol{y},\boldsymbol{z}) \qquad \boldsymbol{f} : \mathbb{R}^k \to \mathbb{R}^m \quad (2)$$

Here $\boldsymbol{x}$ is the vector corresponding to the capacitor voltages and inductor currents, $\boldsymbol{z}$ is the vector corresponding to independent voltages or current sources and $\boldsymbol{y}$ is a vector of additional voltages and currents. $\boldsymbol{B}(\boldsymbol{x})$ is a matrix related to the dynamical elements. If there are nonlinear capacitances or inductances, one approach is to separate $\boldsymbol{B}(\boldsymbol{x})$ in a linear and a nonlinear part. If there are only linear inductances and capacitances $\boldsymbol{B}$ is a constant matrix. We exclude forced degeneracies from our discussion (i.e. meshes of capacitors and cut-sets of inductors, as well as $L(i) = 0$ or $C(u) = 0$) [3], so that $\boldsymbol{B}$ has full rank. Therefore, we can multiply eq. (1) with $\boldsymbol{B}^{-1}$ yielding:

$$\dot{\boldsymbol{x}} = \boldsymbol{g}(\boldsymbol{x},\boldsymbol{y},\boldsymbol{z}) \qquad \boldsymbol{g} : \mathbb{R}^k \to \mathbb{R}^n \quad (3)$$

$\boldsymbol{g}$ represents a nonlinear vector field with respect to $\boldsymbol{x}$, $\boldsymbol{y}$ and $\boldsymbol{z}$. The dimension of the embedding space is k and the state space $\mathcal{S}$ has the dimension $l = n + \eta$, where η is the number of independent input sources.

A. State Space can be viewed as differentiable manifold

We interpret the state space $\mathcal{S}$ of an electronic system as differential manifold (cf. [6]), represented by the solution set of the algebraic equations (2). To find a starting point on the manifold we search for the zero set of the homotopy $H(\boldsymbol{w}, \lambda, \boldsymbol{w_0}) = \boldsymbol{f(w)} + (\lambda - 1)\boldsymbol{f(w_0)}$ ([7], [8]). The point $\boldsymbol{w_0}$ lies somewhere in the embedding space and by differentiating we obtain $\frac{d\boldsymbol{w}}{d\lambda} = -\boldsymbol{J}^{+}\boldsymbol{f(w_0)}$, where $\boldsymbol{J}$ is the Jacobian of $\boldsymbol{f}$ and $\boldsymbol{J}^{+}$ is the pseudo-inverse of $\boldsymbol{J}$. Starting from $\boldsymbol{w}(0) = \boldsymbol{w_0}$ we integrate this equation until we arrive at $\boldsymbol{p} := \boldsymbol{w}(1)$, which is the starting point on the manifold. Given the starting point $\boldsymbol{p} \in \mathcal{S}$, we can parametrize $\mathcal{S}$ with geodesic coordinates by computing geodesic curves from $\boldsymbol{p}$ as shown in [9]. With this parametrization, each point on the manifold can be described by the length and the starting direction of the respective geodesic curve, cf. [3].

B. Jumps in state space

The dynamics of a nonlinear dynamic circuit are defined by the set of all solutions of the differential equations (1) on a sufficient smooth state space $\mathcal{S}$. Therefore $\mathcal{S}$ has to be a smooth manifold and the dynamics have to be created on $\mathcal{S}$. We consider only the generic case, where $\mathcal{S}$ is a smooth manifold (for a detailed discussion cf. [10]). Obtaining the transient response requires the construction of a vector field X on the smooth manifold $\mathcal{S}$ of the circuit. We have shown that X cannot be created on $\mathcal{S}$, when the local solvability to $\boldsymbol{y}$ is not guaranteed: i.e. at the fold edge of $\mathcal{S}$ (cf. [3]).

These points are specified by the following condition:

$$\det\left(\partial_{\boldsymbol{y}}\boldsymbol{f}(\boldsymbol{x},\boldsymbol{y},\boldsymbol{z})\right) = 0 \text{ where } \boldsymbol{f}(\boldsymbol{x},\boldsymbol{y},\boldsymbol{z}) = \boldsymbol{0} \qquad (4)$$

Therefore we assume eq. (4) to be the necessary jump condition, see also [11], [12].

A point that is specified by eq. (4) and whose neighborhood includes each a Lyapunov-stable and -unstable point, is called proper jump point P_j. This sufficient jump condition can be verified by calculating the eigenvalues λ_i of the characteristic equation

$$\det\left(\partial_{\boldsymbol{y}}\boldsymbol{f}(\boldsymbol{x},\boldsymbol{y},\boldsymbol{z}) - \lambda \cdot \boldsymbol{E}\right) = 0\ , \qquad (5)$$

where $\boldsymbol{E}$ is the identity matrix (cf. theory of discontinuous oscillators e.g. [13], [14]). We call the set of all points fulfilling these two conditions "jump-set" Γ. By crossing Γ between stable and unstable region, there appears either one real positive λ or a pair of conjugate complex λ_1, λ_2 with positive real parts. The appearance of more than two λ_i with positive real parts is uncommon and will not be analyzed [13]. We will restrict ourself to the case, where only one real positive λ appears. Then, for points on Γ, there is only one eigenvalue equal to zero. As a result the constant term of eq. (5) (which corresponds to eq. (4) cf. [13]) is equal to zero. Therefore, the necessary and sufficient jump condition can be tested by the zero crossing of the determinant (4).

Tracing the jump-set

We start by tracing geodesics from p in multiple directions. While tracing the geodesics, the jump condition (4) is checked by a local evaluation. Here the sufficient Lyapunov condition is verified by a zero crossing of the determinant. From the first found jump point, we can trace the jump-set $\boldsymbol{\Gamma}(s)$ by following its tangent vector $\boldsymbol{\Gamma}'(s)$. To this end, we differentiate (4) and obtain a linear equation for $\boldsymbol{\Gamma'}$. Together with $\boldsymbol{J\Gamma'} = \boldsymbol{0}$ and $\|\boldsymbol{\Gamma'}\| = 1$, we get a linear equation system that can be solved for $\boldsymbol{\Gamma'}$.

Finding the hit-set

The corresponding "hit-set" Ψ is the intersection of the "bundle" of all jump spaces at points of the jump-set and the state space $\mathcal{S}$. Under the natural physical constraints, the energy of capacitors and the charge of inductors is preserved, such that the voltage across a capacitance or the current through an inductance have inertia through the jump process and do not change (i.e. the values of $\boldsymbol{x}$ do not change during the jump). Another restriction are the fixed values of $\boldsymbol{z}$ during the jump, which additionally reduces the jump space. Therefore, the jump takes place in a subspace parallel to the space given by $\boldsymbol{y}$. Thus the jump direction is predefined and the trajectories "hit" the manifold $\mathcal{S}$. Obviously, for this construction an embedding space is needed. As for the jump-set, an analytical formulation of

the hit-set is barely possible. With our approach, the hit-set is numerical determined by a local data evaluation.
We use a bisection method to find a single point P_h of the hit-set $\mathbf{\Psi}(s)$ corresponding to the actual point P_j of the jump-set $\mathbf{\Gamma}(s)$. This gives us a set of possible points from which we have to choose the one closest to P_j. Another approach is to use a homotopy method. The hit-set can be traced while tracing the jump-set. For this, every tangent vector of the jump-set is translated to the actual position of the hit-set and projected into the tangential space there by using $\mathbf{\Psi'} = \mathbf{\Gamma'} - \boldsymbol{J}^{+}\boldsymbol{J}\mathbf{\Gamma'}$, cf. [15].

C. Tracing the dynamics

To obtain the transient solution, the dynamics $d \in \mathbb{R}^k$ is traced. The trace starts from a given point $\boldsymbol{p} \in \mathcal{S}$ computed as described in section II-A. Of course, every point of the searched curve $\boldsymbol{\eta}(t) = (\boldsymbol{x}(t), \boldsymbol{y}(t), \boldsymbol{z}(t))$ has to lie on the manifold, i.e., $\boldsymbol{f}(\boldsymbol{\eta}(t)) = \boldsymbol{0}$.

If we assume $\boldsymbol{B}$ to be a constant, full rank matrix, so that eq. (3) is valid, the dynamics vector can be determined as $\boldsymbol{d} = (\boldsymbol{g}(\boldsymbol{\eta}(t)), \boldsymbol{0}, \boldsymbol{0})^{\top}$. Alternatively, if $\boldsymbol{B}(\boldsymbol{x})$ is not a constant matrix, we consider the dynamics as a solution of the implicit equation system $\boldsymbol{G}(\boldsymbol{\eta}(t), \boldsymbol{d}) = \boldsymbol{B}(\boldsymbol{x})\dot{\boldsymbol{x}} - \tilde{\boldsymbol{g}}(\boldsymbol{x}, \boldsymbol{y}, \boldsymbol{z}) = 0$ We differentiate this equation with respect to t and solve for $\dot{\boldsymbol{d}}$. We set $\boldsymbol{\eta}$ to the starting point $\boldsymbol{p}$ and determine $\boldsymbol{d}$ with an analog homotopy method (see section II-A). Then we can trace $\boldsymbol{d}$ together with $\boldsymbol{\eta}$. Similar procedures can be found in [7].

Now, the tangential vector $\dot{\boldsymbol{\eta}}(t)$ satisfies $\dot{\boldsymbol{\eta}}(t) = \boldsymbol{P}(\boldsymbol{d})$ where $\boldsymbol{P}$ projects $\boldsymbol{d}$ into the tangential space $T_{\boldsymbol{\eta}}\mathcal{S}$. The projection is calculated as $\boldsymbol{P}(\boldsymbol{d}) = \boldsymbol{d} - \boldsymbol{A}(\boldsymbol{J}\boldsymbol{A})^{-1}\boldsymbol{J}\boldsymbol{d}$ where $\boldsymbol{A}$'s columns span the jump-space given by $\boldsymbol{y}$.

The dynamics $\boldsymbol{d}$ becomes singular in the points of the jump-set Γ and exhibits a high acceleration in its neighborhood. Therefore, the transient solution can be determined by tracing $\boldsymbol{\eta}(t)$ until fulfilling the stopping criterion (4), then choosing the nearest jump point, calculating the corresponding hit point and tracing $\boldsymbol{\eta}(t)$ until reaching Γ again.

III. Application on nonlinear circuits

In previous works [1], [2], [3], we applied our methods to the first three example circuits shown in table III. The abbreviation DES stands for Dimension of Embedding Space, DSS for Dimension of State Space and DJS for Dimension of Jump Space. The first two examples are autonomous circuits with a maximal codimension of 2. The significant sets of $\mathcal{S}$, such as Γ and Ψ, were analyzed with the described differential geometric methods by a local data evaluation in [1] and [3]. For the simulation, only the circuit equations have to be specified. The third excited circuit has a codimension of 4 and was analyzed together with example 2 in [2], but there the jump condition was formulated explicitly and only the regularized system dynamics were traced. With the methods described in this work, there is no limit of a maximal codimension and tracing the dynamics of autonomous circuits without regularization is possible. Only the tracing of the transients of excited circuits is still lacking.

Name of electronic circuit	DES	DSS	DJS
BIP emitter coupled multivibrator	3	1	2
BIP multivibrator with 2 capacitances	4	2	2
BIP Flip Flop	5	1	4
MOS Flip Flop	5	1	4

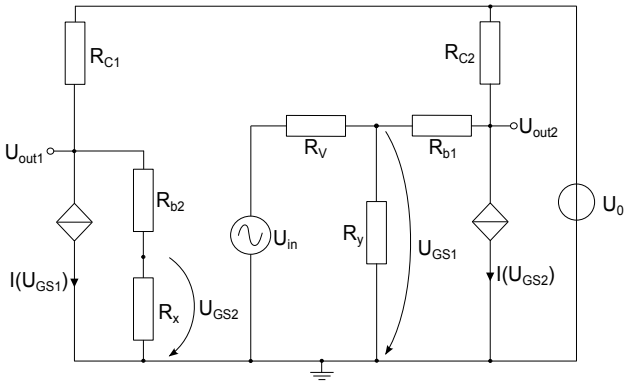

Fig. 1. MOS Flip Flop

Now, we illustrate our concept with a MOS flip flop. To analyze the flip flop circuit illustrated in Fig. 1, we use the EKV model for the drain-source current [16]: $I_{DS} = f(U_{GS}) = a \cdot ln^2\left(1 + e^{b(U_{GS} - V_t)}\right)$, where U_{GS} is the gate source voltage and V_t is the threshold voltage. The design parameters are $R_{C1} = R_{C2} = 10\Omega$, $R_{b1} = R_{b2} = 10k\Omega$, $R_x = 10k\Omega$, $R_y = 20k\Omega$, $R_V = 5k\Omega$ and $U_0 = 9V$. The drain-source current of the transistor was fitted with the parameter-set $a = 1.3mA$, $b = 10.725\frac{1}{V}$ and $V_t = 1.6V$. For the comparison of the non-regularized solution with the solution of the regularized system, the parasitic capacitances C_{reg}

parallel to the gate-source nodes (U_{GS}) were added. The MOS flip flop can be considered as a circuit with three inner state variables $U_{GS1} - U_{GS2} - U_{in}$. These coordinates span the three-dimensional embedding space. Because the value of the input voltage is fixed during the jump, the two-dimensional jump space is parallel to the axis $U_{GS1} - U_{GS2}$ and contains the jump points. One can derive two algebraic constraints by Kirchhoff's law, see eq. (6) and eq. (7), which leads to a one dimensional state space manifold.

$$\frac{U_0}{qR_{b1}R_{c2}} - (k - \frac{1}{qR_{b1}^2})U_{GS1} + \frac{U_{in}}{R_v} = \frac{f(U_{GS2})}{qR_{b1}} \tag{6}$$

$$\frac{U_0}{pR_{c1}R_{b2}} + (\frac{1}{pR_{b2}^2} - \frac{1}{R_{b2}} - \frac{1}{R_x})U_{GS2} = \frac{f(U_{GS1})}{pR_{b2}} \tag{7}$$

Here $k = \frac{1}{R_{b1}} + \frac{1}{R_v} + \frac{1}{R_y}$, $p = \frac{1}{R_{c1}} + \frac{1}{R_{b2}}$, $q = \frac{1}{R_{c2}} + \frac{1}{R_{b1}}$ and U_{in} is the input voltage.
In Fig. 2 the state space (blue) in the $U_{GS1} - U_{GS2} - U_{in}$ coordinate system is shown. The jump paths are marked with green circles, the jump points with blue rectangles, the hit points with yellow rectangles and the trajectories of the regularized system with red triangles. As one can see, the jump and hit points were correctly identified for $C_{reg} = 5fF$. By choosing bigger regularization capacitances, the transient solution will significantly comes off $\mathcal{S}$ at a point $P_{jump,reg}$ before reaching the calculated jump point P_{jump} and will first proceeds in the "near" of $\mathcal{S}$ at $P_{hit,reg}$ instead of P_{hit}. Our studies showed, that the transient solution of the regularized system approaches for $C_{reg} \to 0$ the non regularized case, so that $P_{jump,reg} \to P_{jump}$ and $P_{hit,reg} \to P_{hit}$. Fig. 2 also shows that the jump path calculated by a geometric connection of jump and hit point differ from the path resulting from the regularized system. Resulting from the regularization, the voltages U_{GS1} and U_{GS2} have inertia through the jump process and do not follow the shortest, geometric connection. Nevertheless, the calculated path will allow us to determine the transient solution of the system without adding regularizing capacitances. The example is more sophisticated, if the output voltages U_{out1} and U_{out2} are taken into account. One can derive the following equations describing the output voltages in dependence of the inner state

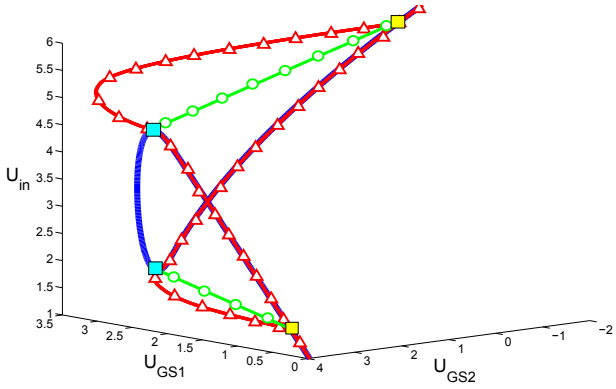

Fig. 2. State space (blue) in $U_{GS1} - U_{GS2} - U_{in}$ coordinate system; jump (green circles); jump point (blue rectangle); hit point (yellow rectangle); path of regularized system (red triangles) for $C_{reg} = 5fF$

variables:

$$\frac{U_0}{pR_{c1}} + \frac{U_{GS2}}{pR_{b2}} - \frac{f(U_{GS1})}{p} - U_{out1} = 0 \tag{8}$$

$$\frac{U_0}{qR_{c2}} + \frac{U_{GS1}}{qR_{b1}} - \frac{f(U_{GS2})}{q} - U_{out2} = 0 \tag{9}$$

The state space manifold remains one dimensional, whereas the embedding space becomes four-dimensional if only eq. (8) is added and five-dimensional when also eq. (9) is taken into account. The jump space in these cases is respectively three or four dimensional. In Fig. 3, the visualization of $\mathcal{S}$ in the 4-dimensional embedding space $U_{GS1} - U_{GS2} - U_{out1} - U_{in}$ is shown. In Fig. 4, $\mathcal{S}$ is shown

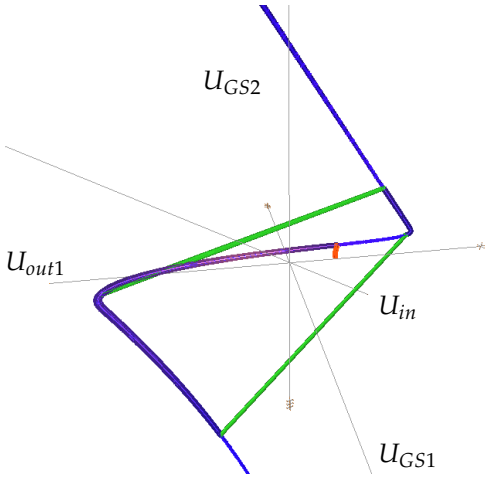

Fig. 3. Visualization of the 4D MOS flip flop in the coordinate system $U_{GS1} - U_{GS2} - U_{out1} - U_{in}$. State space (blue); jumps (green); homotopy path (red)

in the $U_{out1} - U_{out2} - U_{in}$ coordinate system.

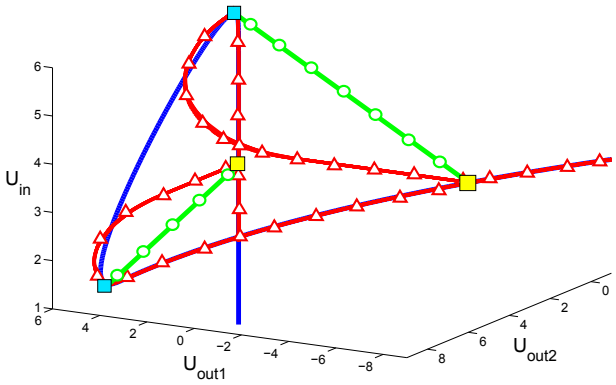

Fig. 4. State space (blue) in $U_{out1} - U_{out2} - U_{in}$ coordinate system; jump (green circles); jump point (blue rectangle); hit point (yellow rectangle); path of regularized system (red triangles) for $C_{reg} = 5fF$

IV. Conclusion

Our approach of directly computing significant sets, i.e., jump- and hit-set, on the state space manifold is able to capture the behavior of circuits with folded state spaces. We want to emphasize, that this approach does not need any regularizing capacitors and inductors. Instead, the describing equation system has to be formulated in a specific way, separating algebraic and differential components. Extending our previous works, we adapted our algorithms to higher dimensions and showed how to trace the dynamics if they are given in the more general implicit form. In the future, we want to assemble parameter studies, observing the behavior of the state space and the traced curves under modification of the circuit parameters.

Acknowledgment

The authors would like to thank the German Research Foundation (DFG) for the financial support.

References

[1] T. Thiessen, M. Gutschke, P. Blanke, W. Mathis, and F.-E. Wolter, "Numerical analysis of relaxation oscillators based on a differential geometric approach," in *International Conference on Signals and Electronic Systems (ICSES 2010)*, Sept. 2010, pp. 209 –212.

[2] T. Thiessen and W. Mathis, "Geometrical interpretation of jump phenomena in nonlinear dynamical circuits," in *Joint 3rd Int'l Workshop on Nonlinear Dynamics and Synchronization (INDS 2011) & 16th Int'l Symposium on Theoretical Electrical Engineering (ISTET 2011)*, july 2011, pp. 1 –5.

[3] T. Thiessen, M. Gutschke, P. Blanke, W. Mathis, and F.-E. Wolter, "A numerical approach for nonlinear dynamical circuits with jumps," in *20th European Conference on Circuit Theory and Design (ECCTD 2011)*, 2011.

[4] A. N. Tikhonov, A. B. Vasil'eva, and A. G. Sveshnikov, *Differential Equations*. Springer-Verlag, 1985.

[5] W. Gear, "Simultaneous numerical solution of differential-algebraic equations," *IEEE Transactions on Circuit Theory*, vol. CT-18, no. 1, pp. 89–95, Jan 1971.

[6] S. Smale, "On the mathematical foundation of electrical circuit theory," *J. Differential Geometry*, vol. 7, no. 1-2, pp. 193–210, 1972.

[7] E. L. Allgower and K. Georg, *Introduction to Numerical Continuation Methods*, ser. Classics in applied mathematics. SIAM, 2003.

[8] W. I. Zangwill and C. B. Garcia, *Pathways to solutions, fixed points, and equilibria*. Prentice-Hall, 1981.

[9] M. do Carmo, *Differential Geometry of Curves and Surfaces*. Prentice-Hall, 1976.

[10] W. Mathis, "Geometric theory of nonlinear dynamical networks," in *Computer Aided Systems Theory EUROCAST – '91*, ser. Lecture Notes in Computer Science, F. Pichler and R. Daz, Eds. Springer, 1992, vol. 585, pp. 52–65.

[11] L. Chua, "Dynamic nonlinear networks: State-of-the-art," *IEEE Transactions on Circuits and Systems*, vol. CAS-27, no. 11, pp. 1059–1087, nov 1980.

[12] R. Nielsen and A. Willson Jr., "A fundamental result concerning the topology of transistor circuits with multiple equilibria," *Proc. of the IEEE*, vol. 68, no. 2, pp. 196 – 208, Feb 1980.

[13] A. A. Andronov, A. A. Vitt, and S. E. Khaikin, *Theory of Oscillators*. Dover Publications Inc., 1987.

[14] E. F. Mishchenko and N. K. Rozov, *Differential Equations with Small Parameters and Relaxation Oscillators*. Plenum Press, 1980.

[15] J. Pegna and F.-E. Wolter, "Surface curve design by orthogonal projection of space curves onto free-form surfaces," *MECH DESIGN*, vol. 118, no. 1, pp. 45–52, Mar. 1996.

[16] C. C. Enz, F. Krummenacher, and E. A. Vittoz, "An analytical mos transistor model valid in all regions of operation and dedicated to low-voltage and low-current applications," *Analog Integr. Circuits Signal Process.*, vol. 8, pp. 83–114, July 1995.